SPANDIDOS PUBLICATIONS

ONCOLOGY REPORTS 29: 751-762, 2013

Smh-3 induces G_2/M arrest and apoptosis through calcium-mediated endoplasmic reticulum stress and mitochondrial signaling in human hepatocellular carcinoma Hep3B cells

CHIN-YU LIU[1], JAI-SING YANG[2], SHIH-MING HUANG[1], JO-HUA CHIANG[4], MING-HUA CHEN[1], LI-JIAU HUANG[1], HO-YU HA[2], SHINJI FUSHIYA[5] and SHENG-CHU KUO[1,3]

[1]Graduate Institute of Pharmaceutical Chemistry, [2]Department of Pharmacology, China Medical University, [3]Chinese Medicine Research and Development Center, China Medical University Hospital, Taichung 404; [4]Department of Life Sciences, National Chung Hsing University, Taichung 402, Taiwan, R.O.C.; [5]Department of Kampo Pharmaceutical Sciences, Nihon Pharmaceutical University, Saitama 362-0806, Japan

Received September 21, 2012; Accepted November 2, 2012

DOI: 10.3892/or.2012.2166

Abstract. In the present study, we investigated the antitumor effects of Smh-3 on the viability, cell cycle and apoptotic cell death in human hepatocellular carcinoma Hep3B cells *in vitro*. We also investigated the molecular mechanisms involved in the effects of Smh-3 on human hepatoma Hep3B cells, including the effects on protein and mRNA levels which were determined by western blotting and DNA microarray methods, respectively. The results demonstrated that Smh-3 induced growth inhibition, cell morphological changes and induction of G_2/M arrest and apoptosis in Hep3B cells. DNA microarray assay identified numerous differentially expressed genes related to angiogenesis, autophagy, calcium-mediated ER stress signaling, cell adhesion, cell cycle and mitosis, cell migration, cytoskeleton organization, DNA damage and repair, mitochondrial-mediated apoptosis and cell signaling pathways. Furthermore, Smh-3 inhibited CDK1 activity, mitochondrial membrane potential ($\Delta\Psi m$) and increased the cytosolic Ca^{2+} release and caspase-4, caspase-9 and caspase-3 activities in Hep3B cells. Western blot analysis demonstrated that Smh-3 increased the protein levels of caspase-4 and GADD153 that may lead to ER stress and consequently apoptosis in Hep3B cells. Taken together, Smh-3 acts against human hepatocellular carcinoma Hep3B cells *in vitro* through G_2/M phase arrest and induction of calcium-mediated ER stress and mitochondrial-dependent apoptotic signaling pathways.

Correspondence to: Professor Sheng-Chu Kuo, Graduate Institute of Pharmaceutical Chemistry, China Medical University, No. 91 Hsueh-Shih Road, Taichung 40402, Taiwan, R.O.C.
E-mail: sckuo@mail.cmu.edu.tw

Key words: Smh-3, G_2/M arrest, apoptosis, endoplasmic reticulum stress, Hep3B cells

Introduction

Cancer is the major cause of mortality in human populations worldwide, and human hepatocellular carcinoma is one of the most lethal types of cancers (1,2). Typical treatment approaches to human hepatocellular carcinoma include hepatic resection, chemotherapy, percutaneous ablation and transcatheter arterial chemoembolization and transplantation, yet patient outcomes are not satisfactory (3,4). Currently, investigators are focusing on new agents and novel targets for human hepatocellular carcinoma treatment (5-7).

Caspases are important proteases in cells. Following apoptotic stimuli, caspases can stimulate intracellular cascades and activate downstream caspase members (8,9). Several apoptotic stimuli have been reported that include extrinsic pathways (receptor-ligand interaction) and intrinsic pathways (mitochondrial-involved) (10-12). In the intrinsic apoptosis pathway, caspase-9 acts as a major initiator caspase, while in the extrinsic pathway, caspase-8 is a major initiator caspase (16-18).

Endoplasmic reticulum (ER) stress induces apoptotic cell death (13-15). Recent studies have identified ER as a third pathway implicated in apoptosis. ER has several biological functions including protein folding, protein trafficking and regulation of the intracellular calcium concentration in apoptosis (15,19,20). When ER disrupts the biological function, the unfolded protein response is triggered and this response occurs through the activation of ER stress sensor proteins, including inositol-requiring enzyme 1 (IRE1), GADD153 and activating transcription factor 6 (ATF-6) (10,11,21). The ubiquitin-proteasome system plays an important role in the degradation of unfolded proteins (22,23). The continued increase of unfolded proteins in the ER lumen disrupts Ca^{2+} homeostasis in the ER and ultimately leads to apoptosis. The major initiator caspase is caspase-4 in human cells or caspase-12 in murine cells (24-26).

In our previous study, we designed and synthesized a series of 2-phenyl-4-quinolone compounds as novel antitumor agents (27-30). 2-(3-(Methylamino)phenyl)-6-(pyrrolidin-1-yl) quinolin-4-one (Smh-3) (Fig. 1A) is a candidate exhibiting the most potential for antitumor activities. We demonstrated that Smh-3 induces G_2/M phase arrest and mitochondrial-dependent apoptotic cell death through inhibition of CDK1 and AKT activity in HL-60 human leukemia cells (31). However, neither the cytotoxic effects of Smh-3 on human hepatocellular carcinoma cells, nor the molecular mechanisms underlying its anticancer activity have been investigated. Therefore, this study investigated the molecular mechanisms of the antitumor effects of Smh-3 on Hep3B cells *in vitro*.

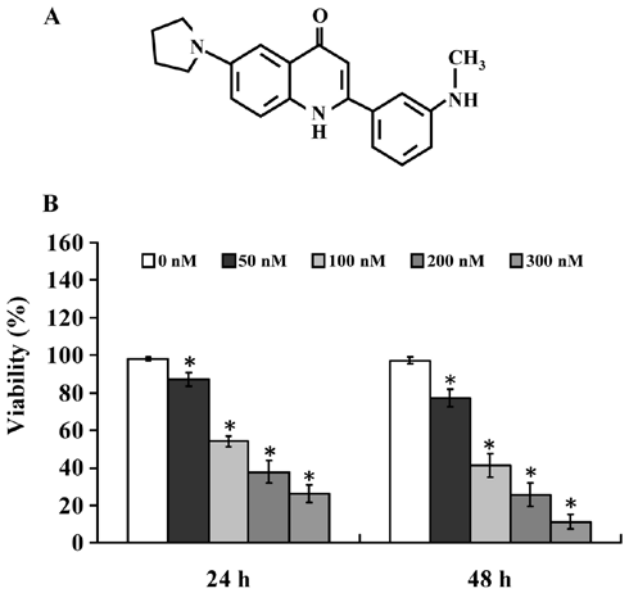

Figure 1. Smh-3 decreases the percentage of Hep3B cell viability. (A) The chemical structure of Smh-3 (2-(3-(methylamino)phenyl)-6-(pyrrolidin-1-yl) quinolin-4-one). (B) Cells were incubated with various concentrations (0, 50, 100, 200 and 300 nM) of Smh-3 for 24 and 48 h and cell viability was determined using an MTT exclusion method. The total number of viable cells was counted using MTT analysis as described in Materials and methods. Each data point is the means ± SD of 3 experiments. *P<0.05.

Materials and methods

Materials, chemicals and reagents. MTT [3-(4,5-dimethylthiazol-2-yl)-2,5-diphenyltetrazolium bromide], potassium phosphate, trypan blue, propidium iodide (PI), Triton X-100, Tris-HCl and ribonuclease-A were obtained from Sigma-Aldrich Corp. (St. Louis, MO). 3'-Dihexyloxacarbocyanine iodide ($DiOC_6$), RPMI-1640 medium, L-glutamine, fetal bovine serum (FBS), Trypsin-EDTA, penicillin, nitrocellulose membrane and the iBlot Dry Blotting system were obtained from Invitrogen Life Technologies (Carlsbad, CA). Caspase-4 activity substrate (Ac-LEVD-pNA) was purchased from BioVision (Mountain View, CA) and caspase-3 and -9 activity assay kits were purchased from R&D Systems (Minneapolis, MN). Primary antibodies (anti-caspase-4, anti-GADD153 and anti-β-actin) and second antibodies for western blotting were obtained from Santa Cruz Biotechnology (Santa Cruz, CA).

Cell culture. The human hepatocellular carcinoma Hep3B cell line was obtained from the Food Industry Research and Development Institute (Hsinchu, Taiwan). The Hep3B cells were incubated in 5% CO_2 at 37˚C in DMEM medium with 2 mM L-glutamine, supplemented with 10% heat-inactivated FBS and 1% antibiotic/antimycotic (100 units/ml penicillin and 100 μg/ml streptomycin) (32).

Determination of cell morphology and the percentage of viable cells. For analysis of cell morphological changes, cells treated with Smh-3 (100 nM) in the well were examined and photographed under a phase-contrast microscope at a magnification of x400. The quantitative analysis of cell viability was performed by MTT assay. Cells ($1x10^4$ cells/well) on 96-well plates were exposed to Smh-3 (0, 50, 100, 200 and 300 nM) and 0.1% DMSO as a vehicle control. After a 24- and 48-h incubation, 100 ml MTT (0.5 mg/ml) solution was added to each well, and the plate was incubated at 37˚C for 4 h. Then, 0.04 N HCl in isopropanol was added, and the absorbance at 570 nm was measured for each well. All results were representative of 3 independent experiments (33,34).

DNA content and cell cycle distribution analysis. Hep3B cells were incubated with 0, 50, 100, 200 and 300 nM of Smh-3 for 24 h. For determination of cell cycle phase and apoptosis, cells were fixed gently in 70% ethanol at -20˚C overnight, and then re-suspended in PBS containing 40 μg/ml PI, 0.1 mg/ml RNase and 0.1% Triton X-100 in a dark room. Cell cycle distribution and apoptotic nuclei were determined by flow cytometry (31,35,36).

CDK1 kinase assay. CDK1 kinase activity was analyzed according to the protocol outlined for the CDK1 kinase assay kit (Medical & Biological Laboratories International, Nagoya, Japan). In brief, the ability of the cell extract prepared from each treatment to phosphorylate its specific substrate, MV peptide, was measured as previously described (31,33).

Caspase activity assay. Hep3B cells were incubated with 0, 50, 100, 200 and 300 nM of Smh-3 for 24 h. Cells were lysed in lysis buffer [50 mM Tris-HCl (pH 7.4), 1 mM EDTA, 10 mM EGTA, 10 mM digitonin and 2 mM DTT]. Approximately 50 μg of cytosol proteins was incubated with caspase-4 (BioVision), caspase-9 and caspase-3-specific substrates (R&D System) for 1 h at 37˚C. The caspase activity was determined by measuring OD_{405} as previously described (31,33,37).

Assay of intracellular Ca^{2+} levels. Hep3B cells were treated with 0, 50, 100, 200 and 300 nM of Smh-3 for 24 h. Cells were harvested, washed twice and re-suspended in 3 mg/ml of Fluo-3/AM (Calbiochem; La Jolla, CA) at 37˚C for 30 min and analyzed by flow cytometry (Becton-Dickinson FACSCalibur) (38,39).

Determination of mitochondrial membrane potential ($\Delta\Psi m$). Hep3B cells were treated with 0, 50, 100, 200 and 300 nM of Smh-3. The cells were harvested and washed twice, resuspended in $DiOC_6$ (4 mmol/l) and incubated for 30 min before being analyzed by flow cytometry (Becton-Dickinson FACSCalibur) (38,39).

Western blot assay. Hep3B cells were placed into 75-T flask. Cells in each well were treated without and with 0, 50, 100, 200 and 300 nM of Smh-3 for 24 h. Cells were collected and total protein from each treatment was extracted and placed into buffer (PRO-PREP™ protein extraction solution, Korea) and centrifuged at 12,000 rpm for 10 min at 4˚C. The quantitated total protein from each treatment was determined by Bradford assay. Proteins from each treatment were resolved on an SDS polyacrylamide gel through electrophoresis (SDS-PAGE) and transferred to nitrocellulose membranes. The membranes were incubated with a blocking buffer of 5% non-fat dry milk in Tris-buffered saline containing Tween-20 for 1 h at room temperature and then incubated with the specific primary antibodies (anti-GADD153 and anti-caspase-4). The membranes were washed and then treated by appropriate horseradish peroxidase (HRP)-conjugated secondary antibodies and visualized using an ECL detection kit (GE Healthcare, Princeton, NJ) (33,40).

cDNA microarray analysis. Hep3B cells were treated with or without 100 nM of Smh-3 for 24 h. Then cells from each treatment were harvested, and the total RNA was extracted using the Qiagen RNeasy Mini kit (Qiagen, Inc., Valencia, CA, USA). The isolated total RNA was used for cDNA synthesis and labeling and microarray hybridization. The fluorescence-labeled cDNA were then hybridized to their complements on the chip (Affymetrix GeneChip Human Gene 1.0 ST array, Affymetrix, Santa Clara, CA, USA). Finally the resulting localized concentrations of fluorescent molecules were detected and quantitated (Asia Bio-Innovations Corp.). The resulting data were analyzed using Expression Console software (Affymetrix) with default RMA parameters. Genes regulated by citosol were determined to have a 1.5-fold change in expression (41).

Statistical analysis. Significance of the mean values between the Smh-3-treated group and control group was obtained using the Student's t-test. Data were expressed as the means ± SD. P<0.05 was considered to indicate a statistically significant difference (33,40).

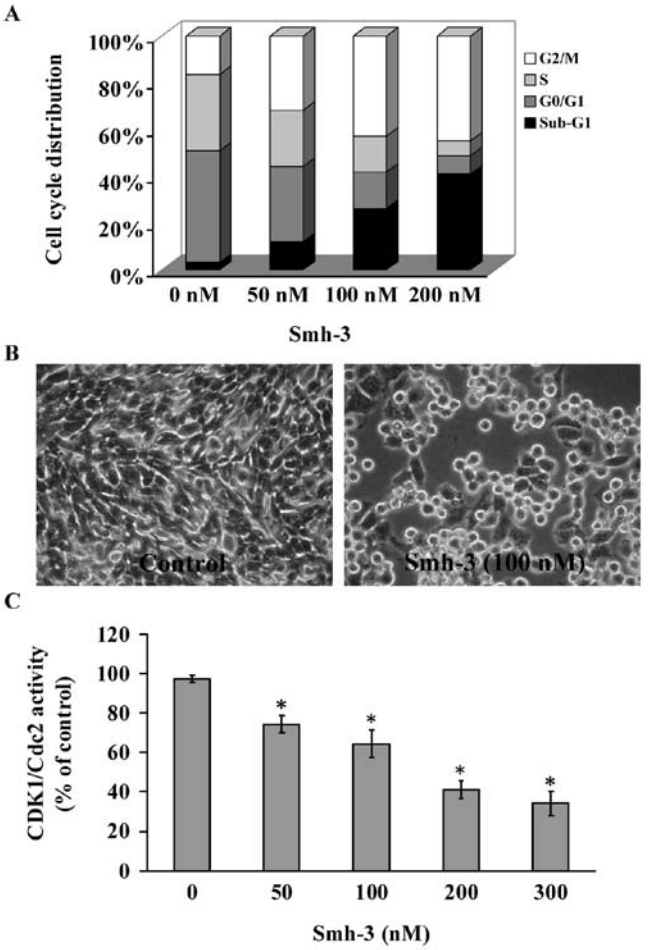

Figure 2. Smh-3 affects cell cycle distribution, cell morphology and CDK1 activity in Hep3B cells. (A) Cells were treated with 0, 50, 100 and 200 nM Smh-3 for 24 h and then harvested for analysis of cell cycle distribution using flow cytometry. Bar graph represents the distribution of Hep3B cells in different phases of the cell cycle. (A) Cells cultured with or without 100 nM of Smh-3 for 24 h were examined for changes in cell morphology and were photographed using a phase-contrast microscope as described in Materials and methods. (C) Cells were treated with 0, 50, 100, 200 and 300 nM of Smh-3 for 24 h and then harvested for analysis of CDK1 activity. Each data point is the means ± SD of 3 experiments. *P<0.05.

Results

Smh-3 decreases the percentage of Hep3B viable cells. To investigate the effect of Smh-3 on cell proliferation, Hep3B cells were treated with 0, 50, 100, 200 and 300 nM of Smh-3 for 48 h. The cell viability following each treatment was analyzed by MTT assay. As shown in Fig. 1B, Smh-3 inhibited Hep3B cell growth in a dose- and time-dependent manner. The half maximal inhibitory concentration IC_{50} following a 48-h treatment of Smh-3 was 68.26±3.24 nM.

Smh-3 induces G_2/M arrest and decreases CDK1 activity and apoptosis in Hep3B cells. Smh-3 induced cell morphological changes and decreased the cell numbers of Hep3B cells (Fig. 2B). Mitotic and apoptotic cells appeared smaller, round and blunt in size following exposure to Smh-3. To investigate the cell cycle distribution of Hep3B cells following Smh-3 treatment, cells were stained with propidium iodide (PI). Flow cytometry revealed that Smh-3 treatment (0, 50, 100 and 200 nM) of Hep3B cells significantly increased the G_2/M cell population at 48 h (Fig. 2A). Furthermore, Smh-3 treatment increased the sub-G_1 cell population at 48 h in a concentration-dependent manner. These data suggest that Smh-3 effectively induces G_2/M arrest and promotes cell death. We examined the CDK1 activity in Smh-3-treated Hep3B cells. Treatment with 0, 50, 100, 200 and 300 nM Smh-3 caused a significant decrease in CDK1 activity (Fig. 2C). Our results suggest that the downregulation of CDK1 activity plays an important role in G_2/M phase arrest in Smh-3-treated Hep3B cells.

cDNA microarray analysis. The microarray analysis indicated 192 genes were upregulated and 278 genes were downregulated in Hep3B cells following treatment with Smh-3. Moreover, the mRNA descriptions of the genes are listed in Table I. DNA microarray assay revealed that many differentially expressed genes related to angiogenesis, autophagy, calcium-mediated ER stress signaling, cell adhesion, cell cycle and mitosis, cell migration, cytoskeleton organization, DNA damage and repair,

Table I. Genes exhibiting more than 1.5-fold changes in mRNA levels in Hep-3B cells following a 24-h treatment with Smh-3 as identified using DNA microarray.

Fold-change	Gene symbol	mRNA description
Biological process: angiogenesis		
1.73	RBPJ	*Homo sapiens* mRNA for H-2K binding factor-2
1.52	GPI	*Homo sapiens* glucose phosphate isomerase
-1.64	SH2D2A	*Homo sapiens* SH2 domain containing 2A
-1.74	RNH1	*Homo sapiens* ribonuclease/angiogenin inhibitor 1
-1.79	RTN4	*Homo sapiens* reticulon 4
-1.87	VEGFA	*Homo sapiens* vascular endothelial growth factor A
Biological process: apoptosis and anti-apoptosis		
1.73	PERP	*Homo sapiens* PERP, TP53 apoptosis effector
1.61	BTG1	*Homo sapiens* B-cell translocation gene 1
1.59	DBH	*Homo sapiens* dopamine β-hydroxylase
1.58	PARP11	*Homo sapiens* poly(ADP-ribose)polymerase family, member 11
1.58	SEMA3A	*Homo sapiens* sema domain
-1.51	ABR	*Homo sapiens* active BCR-related gene
-1.51	BLOC1S2	*Homo sapiens* biogenesis of lysosomal organelles complex-1
-1.51	BCL2L1	*Homo sapiens* BCL2-like 1
-1.52	CARD17	*Homo sapiens* caspase recruitment domain family, member 17
-1.53	YARS	*Homo sapiens* tyrosyl-tRNA synthetase
-1.54	USP17L2	*Homo sapiens* ubiquitin specific peptidase 17-like 2
-1.56	APH1B	*Homo sapiens* anterior pharynx defective 1 homolog B
-1.62	IHH	*Homo sapiens* Indian hedgehog homolog
-1.75	CIDEB	*Homo sapiens* cell death-inducing DFFA-like effector b
-1.85	BCL6	*Homo sapiens* B-cell CLL/lymphoma 6, transcript variant 1
Biological process: autophagy		
1.97	ATG12	*Homo sapiens* ATG12 autophagy related 12 homolog
1.85	CLEC4F	*Homo sapiens* C-type lectin domain family 4, member F
1.64	ACP2	*Homo sapiens* acid phosphatase 2, lysosomal
1.55	HPS1	*Homo sapiens* Hermansky-Pudlak syndrome 1
1.53	NEU1	*Homo sapiens* sialidase 1
1.51	GABARAP	*Homo sapiens* GABA receptor-associated protein
-1.62	CHIT1	*Homo sapiens* chitinase 1
-1.68	VPS53	*Homo sapiens* vacuolar protein sorting 53 homolog
-2.12	SYT3	*Homo sapiens* synaptotagmin III
Biological process: calcium-mediated signaling		
1.68	CCL3	*Homo sapiens* chemokine ligand 3
1.66	STC1	*Homo sapiens* stanniocalcin 1
1.53	CHRNA10	*Homo sapiens* cholinergic receptor
1.53	GRIN1	*Homo sapiens* glutamate receptor
1.50	ETNK2	*Homo sapiens* ethanolamine kinase 2
-1.50	CX3CL1	*Homo sapiens* chemokine ligand 1
-1.52	PLCG2	*Homo sapiens* phospholipase C, γ 2
-1.55	NMUR1	*Homo sapiens* neuromedin U receptor 1
-1.64	CALCB	*Homo sapiens* calcitonin-related polypeptide β
-2.43	KCNA5	*Homo sapiens* potassium voltage-gated channel
Biological process: cell adhesion		
2.50	PVRL2	*Homo sapiens* poliovirus receptor-related 2
1.71	SYMPK	*Homo sapiens* symplekin
1.68	SIGLEC5	*Homo sapiens* sialic acid binding Ig-like lectin 5
1.63	LPXN	*Homo sapiens* leupaxin

Table I. Continued.

Fold-change	Gene symbol	mRNA description
Biological process: cell adhesion		
1.63	CDH6	*Homo sapiens* cadherin 6
1.56	GPR56	*Homo sapiens* G protein-coupled receptor 56
-1.50	PVRL4	*Homo sapiens* poliovirus receptor-related 4
-1.51	SIGLEC14	*Homo sapiens* sialic acid binding Ig-like lectin 14
-1.51	CPXM2	*Homo sapiens* carboxypeptidase X, member 2
-1.52	MMRN1	*Homo sapiens* multimerin 1
-1.53	NCAM1	*Homo sapiens* neural cell adhesion molecule 1
-1.54	PCDHB4	*Homo sapiens* protocadherin β 4
-1.54	PCDHB14	*Homo sapiens* protocadherin β 14
-1.58	PCDHB13	*Homo sapiens* protocadherin β 13
-1.58	PXN	*Homo sapiens* paxillin
-1.61	HSPB11	*Homo sapiens* heat shock protein family B
-1.61	ITGA7	*Homo sapiens* integrin, α 7
-1.62	SIRPG	*Homo sapiens* signal-regulatory protein γ
-1.62	NINJ2	*Homo sapiens* ninjurin 2
-1.62	NEO1	*Homo sapiens* neogenin homolog 1
-1.68	CYR61	*Homo sapiens* cysteine-rich, angiogenic inducer, 61
Biological process: cell cycle and mitosis		
2.13	CNNM3	*Homo sapiens* cyclin M3
1.84	RAB11B	*Homo sapiens* RAB11B, member RAS oncogene family
1.80	CDKN3	*Homo sapiens* cyclin-dependent kinase inhibitor 3
1.64	40789	*Homo sapiens* septin 3
1.59	MGC16703	*Homo sapiens* tubulin, α pseudogene
1.55	KRT18	*Homo sapiens* keratin 18
1.52	ARL8B	*Homo sapiens* ADP-ribosylation factor-like 8B
1.52	RPRM	*Homo sapiens* reprimo, TP53 dependent G2 arrest mediator candidate
-1.50	HAUS6	*Homo sapiens* HAUS augmin-like complex, subunit 6
-1.52	HSPA8	*Homo sapiens* heat shock 70 kDa protein 8
-1.55	ACLY	*Homo sapiens* ATP citrate lyase
-1.57	CCNG1	*Homo sapiens* cyclin G1
-1.62	CHEK2	*Homo sapiens* CHK2 checkpoint homolog
-1.63	TAF1	*Homo sapiens* TAF1 RNA polymerase II
-1.73	PHF16	*Homo sapiens* PHD finger protein 16
-1.87	DUSP1	*Homo sapiens* dual specificity phosphatase 1
-1.89	PISD	*Homo sapiens* THAP domain containing, apoptosis associated protein 1
-1.96	CLPX	*Homo sapiens* non-SMC condensin I complex, subunit H
-2.10	SLC25A26	*Homo sapiens* septin 2
Biological process: cell migration		
-1.54	PLXNB1	*Homo sapiens* plexin B1
-1.56	CLIC4	*Homo sapiens* chloride intracellular channel 4
-1.66	RNF20	*Homo sapiens* ring finger protein 20
-1.72	S100A2	*Homo sapiens* S100 calcium binding protein A2
-1.73	SEMA3C	*Homo sapiens* sema domain, immunoglobulin domain, short basic domain
Biological process: cytoskeleton organization and mitosis		
2.19	TPM3	*Homo sapiens* tropomyosin 3
1.63	CHD2	*Homo sapiens* chromodomain helicase DNA binding protein 2
1.59	CORO2A	*Homo sapiens* coronin, actin binding protein, 2A
1.59	ARHGAP26	*Homo sapiens* Rho GTPase activating protein 26
1.59	DSTN	*Homo sapiens* destrin (actin depolymerizing factor)
1.57	ACTB	*Homo sapiens* actin

Table I. Continued.

Fold-change	Gene symbol	mRNA description
Biological process: cytoskeleton organization and mitosis		
1.57	ACTG1	*Homo sapiens* actin, γ 1
1.56	TUBA1B	*Homo sapiens* tubulin, α 1b
1.51	TUBB2C	*Homo sapiens* tubulin, β 2C
1.50	KIF21A	*Homo sapiens* kinesin family member 21A
-1.51	KIF19	*Homo sapiens* kinesin family member 19
-1.51	MC1R	*Homo sapiens* melanocortin 1 receptor
-1.51	RUVBL1	*Homo sapiens* RuvB-like 1
-1.53	NDE1	*Homo sapiens* nudE nuclear distribution gene E homolog 1
-1.58	C2CD3	*Homo sapiens* C2 calcium-dependent domain containing 3
-1.59	NXF5	*Homo sapiens* nuclear RNA export factor 5
-1.70	BICD2	*Homo sapiens* bicaudal D homolog 2
-1.76	CYP1A1	*Homo sapiens* cytochrome P450, family 1, subfamily A, polypeptide 1
-1.88	MAP1B	*Homo sapiens* microtubule-associated protein 1B
-1.95	KRT1	*Homo sapiens* keratin 1
Biological process: DNA damage and repair		
2.53	NPM1	*Homo sapiens* nucleophosmin
1.93	DDIT3	*Homo sapiens* DNA-damage-inducible transcript 3
1.80	BRCC3	*Homo sapiens* BRCA1/BRCA2-containing complex, subunit 3
1.56	FTO	*Homo sapiens* fat mass and obesity associated
1.52	HIPK1	*Homo sapiens* homeodomain interacting protein kinase 1
-1.54	MRPS11	*Homo sapiens* mitochondrial ribosomal protein S11
-1.54	GNL1	*Homo sapiens* guanine nucleotide binding protein-like 1
-1.57	NAA10	*Homo sapiens* N(α)-acetyltransferase 10, NatA catalytic subunit
-1.58	MORF4L2	*Homo sapiens* mortality factor 4 like 2
-1.59	ATRX	*Homo sapiens* α thalassemia/mental retardation syndrome X-linked
-1.59	RUVBL2	*Homo sapiens* RuvB-like 2
-1.63	NCOA6	*Homo sapiens* nuclear receptor coactivator 6
-1.72	POLB	*Homo sapiens* polymerase, β
-1.83	ATMIN	*Homo sapiens* ATM interactor
-2.03	CIRBP	*Homo sapiens* cold inducible RNA binding protein
-2.78	SGK3	*Homo sapiens* serum/glucocorticoid regulated kinase family, member 3
Biological process: DNA transcription and replication		
1.96	GLI1	*Homo sapiens* GLI family zinc finger 1
1.58	CDC7	*Homo sapiens* cell division cycle 7 homolog
1.53	SET	*Homo sapiens* SET nuclear oncogene
-1.55	MCM6	*Homo sapiens* minichromosome maintenance complex component 6
-1.59	THRA	*Homo sapiens* thyroid hormone receptor, α
-1.67	NOBOX	*Homo sapiens* NOBOX oogenesis homeobox
Biological process: ER function and ER stress		
1.78	NECAB1	*Homo sapiens* N-terminal EF-hand calcium binding protein1
1.77	EFCAB4B	*Homo sapiens* EF-hand calcium binding domain 4B
1.71	CHRNA7	*Homo sapiens* cholinergic receptor, nicotinic, α 7
1.65	RYR1	*Homo sapiens* ryanodine receptor 1
1.63	GRIN2A	*Homo sapiens* glutamate receptor
1.61	SNAP25	*Homo sapiens* synaptosomal-associated protein
1.53	ALG13	*Homo sapiens* asparagine-linked glycosylation 13 homolog
1.53	MLEC	*Homo sapiens* malectin
1.51	CYP2B6	*Homo sapiens* cytochrome P450, family 2, subfamily B, polypeptide 6
-1.50	UBQLN4	*Homo sapiens* ubiquilin 4
-1.50	FITM1	*Homo sapiens* fat storage-inducing transmembrane protein 1

Table I. Continued.

Fold-change	Gene symbol	mRNA description
Biological process: ER function and ER stress		
-1.55	SEC22B	*Homo sapiens* SEC22 vesicle trafficking protein homolog B
-1.55	DERL1	*Homo sapiens* Der1-like domain family, member 1
-1.63	FOXRED2	*Homo sapiens* FAD-dependent oxidoreductase domain containing 2
-1.63	CYP4A22	*Homo sapiens* cytochrome P450, family 4, subfamily A, polypeptide 22
-1.69	PLA2G2A	*Homo sapiens* phospholipase A2, group IIA
-1.72	HSP90B2P	*Homo sapiens* heat shock protein 94b
-2.36	NOX4	*Homo sapiens* NADPH oxidase 4
-4.84	S100A7	*Homo sapiens* S100 calcium binding protein A7
Biological process: mitochondrial function		
1.91	ACAD8	*Homo sapiens* 5-methyltetrahydrofolate-homocysteine methyltransferase reductase
1.74	ACOT2	*Homo sapiens* ATP synthase, H^+ transporting, mitochondrial F0 complex
1.73	SPNS1	*Homo sapiens* MpV17 mitochondrial inner membrane protein
1.72	NMRAL1	*Homo sapiens* NmrA-like family domain containing 1, mitochondrial
1.69	ACSS2	*Homo sapiens* NADH dehydrogenase 1 β subcomplex, 4, 15 kDa
1.68	SAT2	*Homo sapiens* cytochrome P450, family 2, subfamily D, polypeptide 6
1.56	MTRR	*Homo sapiens* cytochrome b-561
1.54	ATP5J	*Homo sapiens* potassium inwardly-rectifying channel
1.52	MPV17	*Homo sapiens* pyruvate dehydrogenase phosphatase regulatory subunit
1.50	LONP1	*Homo sapiens* solute carrier family 3, member 1
-1.50	NDUFB4	*Homo sapiens* thymidine phosphorylase
-1.54	CYP2D6	*Homo sapiens* dynamin 1-like
-1.55	CYB561	*Homo sapiens* solute carrier family 25, member 30
-1.57	KCNJ11	*Homo sapiens* MOCO sulphurase C-terminal domain containing 2
-1.58	PDPR	*Homo sapiens* cytochrome c oxidase subunit VIb polypeptide 1
-1.59	SLC3A1	*Homo sapiens* phosphatidylserine decarboxylase
-1.62	TYMP	*Homo sapiens* ClpX caseinolytic peptidase X homolog
-1.62	DNM1L	*Homo sapiens* solute carrier family 25, member 26
-1.64	SLC25A30	*Homo sapiens* yrdC domain containing
-1.65	MOSC2	*Homo sapiens* surfeit 1
-2.10	COX6B1	*Homo sapiens* cytochrome P450, family 27, subfamily C, polypeptide 1
Biological process: cell signal transduction		
2.54	ZCCHC8	*Homo sapiens* Rho GTPase activating protein 12
2.18	DHX35	*Homo sapiens* cannabinoid receptor 2
2.12	DGCR14	*Homo sapiens* guanine nucleotide binding protein
2.08	RPS13	*Homo sapiens* calcitonin-related polypeptide α
1.97	SNRPG	*Homo sapiens* opsin 4
1.83	RBMY1A1	*Homo sapiens* growth factor receptor-bound protein 10
1.83	ARHGAP12	*Homo sapiens* ribosomal protein S6 kinase, 90 kDa, polypeptide 3
1.80	CNR2	*Homo sapiens* prolactin
1.78	GNAO1	*Homo sapiens* ras homolog gene family, member G
1.77	CALCA	*Homo sapiens* leukocyte-associated immunoglobulin-like receptor 2
1.75	OPN4	*Homo sapiens* CD79b molecule, immunoglobulin-associated β
1.74	GRB10	*Homo sapiens* leukocyte immunoglobulin-like receptor
1.74	RPS6KA3	*Homo sapiens* CD28 molecule
1.69	PRL	*Homo sapiens* A kinase anchor protein 3
1.69	RHOG	*Homo sapiens* RAB6C
1.68	LAIR2	*Homo sapiens* RAB41
1.66	CD79B	*Homo sapiens* RAB15
1.66	LILRB2	*Homo sapiens* ras homolog gene family, member V
1.65	CD28	*Homo sapiens* RAB, member of RAS oncogene family-like 2A

Table I. Continued.

Fold-change	Gene symbol	mRNA description
Biological process: cell signal transduction		
1.65	AKAP3	*Homo sapiens* RAB, member of RAS oncogene family-like 2B
1.65	RAB6C	*Homo sapiens* RAB43, member RAS oncogene family
1.63	RAB41	*Homo sapiens* leukemia inhibitory factor
1.63	RAB15	*Homo sapiens* CD81 molecule
1.62	RHOV	*Homo sapiens* CD74 molecule
1.59	RABL2A	*Homo sapiens*s transforming growth factor, β 3
1.59	RABL2B	*Homo sapiens* sema domain
1.58	RAB43	*Homo sapiens* acylglycerol kinase
1.56	LIF	*Homo sapiens* pleckstrin and Sec7 domain containing
1.56	CD81	*Homo sapiens* fibroblast growth factor binding protein 1
1.54	CD74	*Homo sapiens* olfactory receptor
1.53	TGFB3	*Homo sapiens* vomeronasal 1 receptor 3
1.53	SEMA4C	*Homo sapiens* olfactory receptor
1.52	AGK	*Homo sapiens* olfactory receptor
1.52	PSD	*Homo sapiens* olfactory receptor
1.51	FGFBP1	*Homo sapiens* olfactory receptor
1.51	OR51A4	*Homo sapiens* taste receptor
1.51	VN1R3	*Homo sapiens* olfactory receptor
-1.50	OR5M10	*Homo sapiens* olfactory receptor
-1.51	OR52N1	*Homo sapiens* neuromedin B receptor
-1.51	OR1B1	*Homo sapiens* G protein-coupled receptor 120
-1.52	OR3A3	*Homo sapiens* olfactory receptor
-1.52	TAS2R1	*Homo sapiens* olfactory receptor
-1.53	OR3A1	*Homo sapiens* olfactory receptor
-1.53	OR1D5	*Homo sapiens* olfactory receptor
-1.53	NMBR	*Homo sapiens* MAS-related GPR, member X2
-1.54	GPR120	*Homo sapiens* G protein-coupled receptor 119
-1.54	OR10C1	*Homo sapiens* olfactory receptor
-1.54	OR10H5	*Homo sapiens* G protein-coupled receptor 109B
-1.55	OR10G4	*Homo sapiens* G protein-coupled receptor 83
-1.56	OR4D5	*Homo sapiens* G protein-coupled receptor 39
-1.56	MRGPRX2	*Homo sapiens* olfactory receptor
-1.56	GPR119	*Homo sapiens* olfactory receptor
-1.57	OR7C2	*Homo sapiens* insulin receptor substrate 1
-1.57	GPR109B	*Homo sapiens* insulin-like 3
-1.58	GPR83	*Homo sapiens* FYN binding protein
-1.58	GPR39	*Homo sapiens* dual specificity phosphatase 16
-1.59	OR2L13	*Homo sapiens* hypocretin receptor 1
-1.62	OR52A1	*Homo sapiens* secretogranin V
-1.63	IRS1	*Homo sapiens* GRB2-related adaptor protein
-1.63	INSL3	*Homo sapiens* regulatory factor X-associated ankyrin-containing protein
-1.66	FYB	*Homo sapiens* ubiquitin specific peptidase 8
-1.69	DUSP16	*Homo sapiens* syndecan binding protein
-1.72	HCRTR1	*Homo sapiens* discoidin domain receptor tyrosine kinase 2
-1.72	SCG5	*Homo sapiens* AXL receptor tyrosine kinase
-1.74	GRAP	*Homo sapiens* adenylate cyclase activating polypeptide 1
-1.75	RFXANK	*Homo sapiens* EPH receptor A8

Table I. Continued.

Fold-change	Gene symbol	mRNA description
Biological process: cell signal transduction		
-1.75	USP8	*Homo sapiens* TBC1D30 mRNA for TBC1 domain family, member 30
-1.75	SDCBP	*Homo sapiens* Rho guanine nucleotide exchange factor
-1.77	DDR2	*Homo sapiens* RAS p21 protein activator 4
-1.78	AXL	*Homo sapiens* RAS-like, family 12
-1.78	ADCYAP1	*Homo sapiens* mediator complex subunit 13
-1.82	EPHA8	*Homo sapiens* mitogen-activated protein kinase kinase 7
-1.92	TBC1D30	*Homo sapiens* dishevelled, dsh homolog 3
-2.28	ARHGEF10	*Homo sapiens* LIM domain binding 1
-3.04	RASA4	*Homo sapiens* coiled-coil domain containing 88C

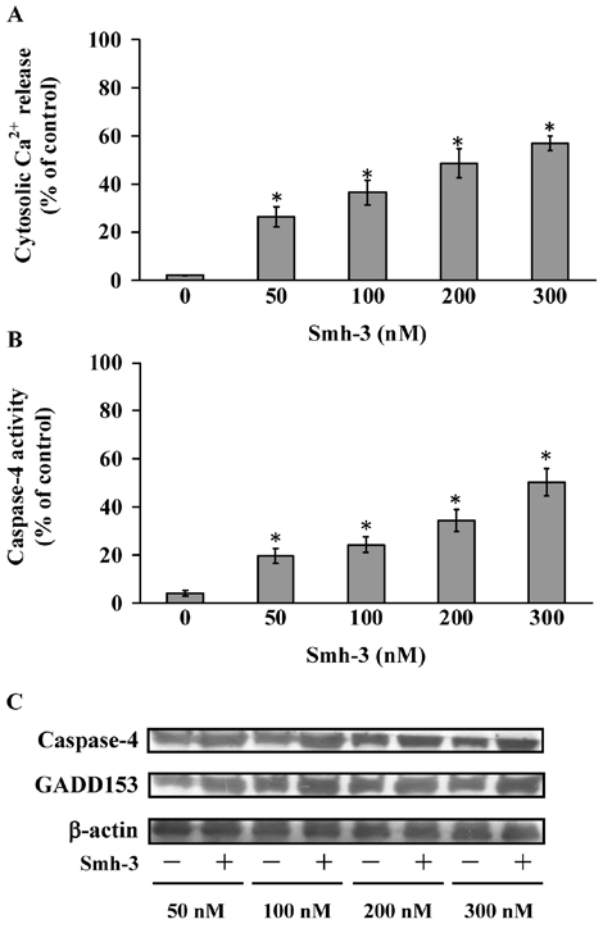

Figure 3. Effects of Smh-3 on ER stress in Hep3B cells. (A) Cells were treated with 0, 50, 100, 200 and 300 nM of Smh-3 for 24 h and the intracellular Ca^{2+} levels were measured using flow cytometric analysis. (B) Cells were treated with 0, 50, 100, 200 and 300 nM of Smh-3 for 24 h and the whole cell lysates were subjected to caspase-4 activity assay. Each data point is the means ± SD of 3 experiments. *P<0.05. (C) Cells were treated with 0, 50, 100, 200 and 300 nM of Smh-3 for 24 h, and whole cell lysate were prepared and the caspase-4 and GADD153 protein levels were estimated by western blotting as described in Materials and methods.

mitochondrial-mediated apoptosis and cell signaling pathways were present in the Hep3B cells following Smh-3 treatment.

Effects of Smh-3 on ER stress in Hep3B cells. Our previous research demonstrated that Smh-3 acts against HL-60 leukemia cells *in vitro* via G_2/M phase arrest, downregulation of AKT activity and induction of mitochondrial-dependent apoptotic pathways (31). To confirm the possibility that the Smh-3-induced apoptosis could be related to contributions from the ER stress signal pathways, Hep3B cells were treated with 0, 50, 100, 200 and 300 nM of Smh-3 for 24 h. The intracellular Ca^{2+} release, caspase-4 activity and the levels of ER stress-associated proteins were examined. The quantities and results are shown in Fig. 3. Results from the flow cytometric assay indicated that Smh-3 induced the production of intracellular Ca^{2+} release (Fig. 3A). To evaluate whether or not Smh-3-induced apoptosis is involved in activation of caspase-4, we determined the caspase-4 activity using caspase colorimetric analysis. Smh-3 at concentrations of 0, 50, 100, 200 and 300 nM stimulated caspase-4 activity in a concentration-dependent manner Fig. 3B. It was reported that GADD153 is a hallmark of ER stress (42,43). Smh-3-treated Hep3B cells were harvested for western blot analysis of the expression levels of the ER stress pathway-related GADD153 and caspase-4 proteins. Smh-3 promoted the protein levels of GADD153 and caspase-4 (Fig. 3C). Based on these results, we suggest that Smh-3-induced apoptosis in Hep3B cells may be mediated through the ER stress-dependent apoptotic signaling pathway.

Effects of Smh-3 on the loss of ΔΨm level, caspase-9 and caspase-3 activities in Hep3B cells. To confirm the possibility that Smh-3-induced apoptosis is related to contributions from the mitochondrial signal pathways, Hep3B cells were treated with 0, 50, 100, 200 and 300 nM of Smh-3 for 24 h, and changes in ΔΨm, caspase-9 and caspase-3 activities were examined; the quantities and results are shown in Fig. 4. Results from the flow cytometric assay indicated that Smh-3 decreased the level of ΔΨm (Fig. 4A). To evaluate whether or not Smh-3-induced apoptosis is involved in activation of caspase-9 and caspase-3, we detected the caspase-9 and caspase-3 activities using caspase colorimetric analysis. Concentrations of 0, 50, 100, 200 and 300 nM of Smh-3 stimulated caspase-9 activity (Fig. 4B) and caspase-3 activity (Fig. 4C) in a concentration-dependent manner.

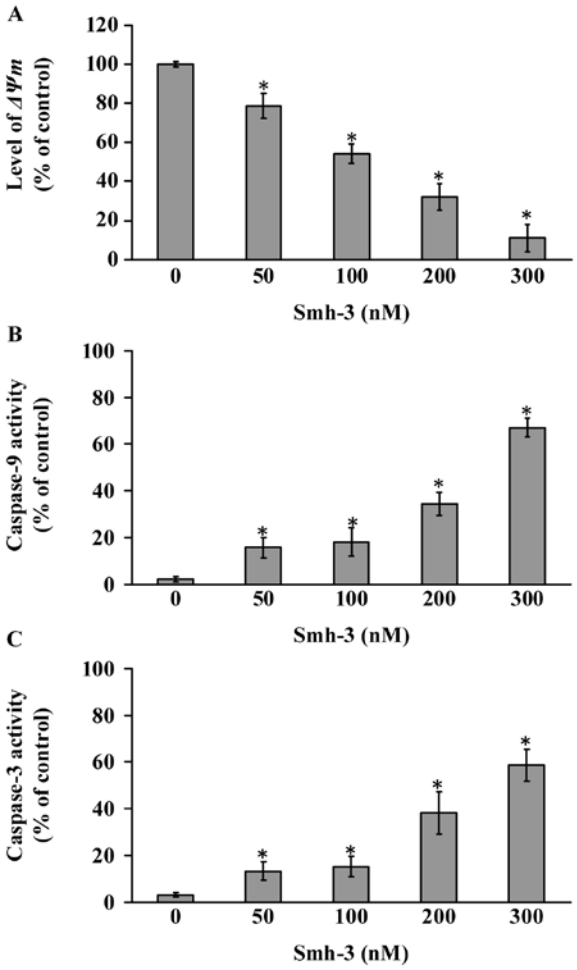

Figure 4. Effects of Smh-3 on the mitochondrial-dependent apoptotic pathway in Hep3B cells. (A) Cells were treated with 0, 50, 100, 200 and 300 nM of Smh-3 for 24 h, and the mitochondrial membrane potential (ΔΨm) was measured by staining with $DiOC_6$. Cells were treated with 0, 50, 100, 200 and 300 nM of Smh-3 for 24 h, and the whole cell lysates were subjected to caspase-9 (B) and caspase-3 (C) activity assay as described in Materials and methods. Each data point is the means ± SD of 3 experiments. *P<0.05.

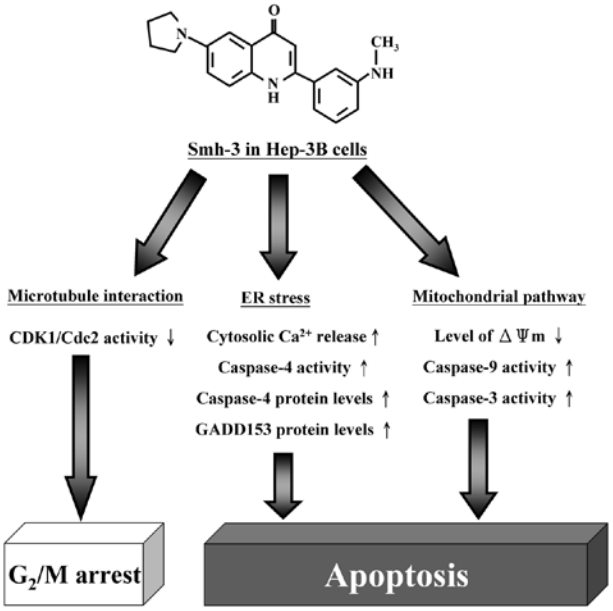

Figure 5. A proposed model and the overall possible signaling pathways involved in the Smh-3-induced apoptosis in Hep3B cells.

Discussion

There are no reports concerning the effects of Smh-3 on apoptosis and associated gene expression in Hep3B cells. The present study is the first to show that Smh-3 induces a cytotoxic effect which includes induction of G_2/M phase arrest and apoptosis and changes in the expression of associated gene in Hep3B cells. In previous studies, we showed that Smh-3 triggered apoptosis in HL-60 human leukemia cells (31); however, the involvement of ER stress in Smh-3-induced apoptosis in cancer cells is still unclear. Our results demonstrated that Smh-3 treatment increased the protein levels of caspase-4 and GADD153 in Hep3B cells (Fig. 3B and C). Our novel findings suggest that these events demonstrate that the ER stress apoptotic pathway is involved in the Smh-3 effects *in vitro*. It has been reported that cellular organelles such as mitochondria, ER, lysosomes and Golgi apparatus are also major targets of apoptotic initiation (44,45). Many chemotherapy agents that strongly affect the function of the ER are identified as strong inducers of GADD153. This suggests that increased intracellular Ca^{2+} induces mitochondrial swelling (39,46). Following mitochondrial permeabilization, cytochrome *c*, Apaf-1, procaspase-9, Endo G and AIF are released into the cytosol, activating caspase-3 via caspase-9 (47,48). Smh-3 induced the activation of caspase-9 and caspase-3 after a 48-h treatment (Fig. 4B and C), suggesting that Smh-3 possibly activates the mitochondrial signaling pathway. Our results demonstrated that Smh-3 decreased the ΔΨm after a 24 h treatment with Smh-3 (Fig. 4A), and then promoted caspase-9 and caspase-3 activities in Hep3B cells (Fig. 4B and C). In addition, caspase-8 activity exhibited no significant increase in the Smh-3-treated Hep3B cells (data not shown). Based on the above evidence, Smh-3-stimulated apoptotic cell death is involved in the cross-talk between the ER and mitochondria.

Based on the change in gene expression profile in Smh-3-treated Hep3B cells by DNA microarray, we found that cellular and molecular responses to Smh-3 treatment are multifaceted and are likely to be mediated via a variety of regulatory pathways. Smh-3 regulated the expression of important genes that control cell growth, angiogenesis, autophagy, calcium-mediated ER stress signaling, cell adhesion, cell cycle and mitosis, cell migration, cytoskeleton organization, DNA damage and repair, mitochondrial-mediated apoptosis, transcription and translation and cell signaling pathways (Table I). Regulation of these genes may be responsible for inhibiting the proliferation of Hep3B cells. It was reported that cyclins associate with cyclin-dependent protein kinases (CDKs) and CDK inhibitor (CKI) to control the process of the cell cycle. The CDK inhibitor (CKI) has been demonstrated to arrest the cell cycle and inhibit the cell growth of cancer cells (33,40,46). From a gene expression profile, we found that Smh-3 altered the expression of cyclin and cyclin-dependent kinase inhibitors and cytoskeleton organization genes including CNNM3, CDKN3, RPRM, CCNG1, ACTB, ACTG1, TUBA1B, TUBB2C and MAP1B, suggesting a change in cyclin, cyclin-dependent kinase inhibitors, and microtubule interaction which could finally lead to cell cycle G_2/M arrest (Fig. 2B).

In conclusion, the molecular signaling pathways involved in Smh-3 effects on Hep-3B cells are summarized in Fig. 5. Based on these data, further detailed investigations including anti-metastasis, anti-angiogenesis and autophagy induction studies are required in order to establish cause and effect relationships between these altered genes and the outcome of human hepatocellular carcinoma patients.

Acknowledgements

The study was supported by research grants from the National Science Council of P.R. China awarded to S.-C.K. (NSC 100-2320-B-039-001) and Taiwan Department of Health, China Medical University Hospital Cancer Research Center of Excellence (DOH101-TD-C-111-005).

References

1. Moriguchi M, Takayama T, Higaki T, *et al*: Early cancer-related death after resection of hepatocellular carcinoma. Surgery 151: 232-237, 2012.
2. Chen TH, Chen CJ, Yen MF, *et al*: Ultrasound screening and risk factors for death from hepatocellular carcinoma in a high risk group in Taiwan. Int J Cancer 98: 257-261, 2002.
3. Ueda H, Fukuchi H and Tanaka C: Toxicity and efficacy of hepatic arterial infusion chemotherapy for advanced hepatocellular carcinoma (Review). Oncol Lett 3: 259-263, 2012.
4. Blum HE: Hepatocellular carcinoma: HCC. Hepat Mon 11: 69-70, 2011.
5. Abou-Alfa GK: New agents in hepatocellular carcinoma. Clin Adv Hematol Oncol 6: 423-424, 2008.
6. Marquardt JU, Galle PR and Teufel A: Hepatocellular carcinoma: molecular pathogenesis and novel targets for therapy. Dtsch Med Wochenschr 137: 855-860, 2012 (In German).
7. Hoshida Y, Toffanin S, Lachenmayer A, Villanueva A, Minguez B and Llovet JM: Molecular classification and novel targets in hepatocellular carcinoma: recent advancements. Semin Liver Dis 30: 35-51, 2010.
8. Chai F, Truong-Tran AQ, Ho LH and Zalewski PD: Regulation of caspase activation and apoptosis by cellular zinc fluxes and zinc deprivation: a review. Immunol Cell Biol 77: 272-278, 1999.
9. Crawford ED, Seaman JE, Barber AE II, *et al*: Conservation of caspase substrates across metazoans suggests hierarchical importance of signaling pathways over specific targets and cleavage site motifs in apoptosis. Cell Death Differ: Aug 24, 2012 (Epub ahead of print).
10. Oyadomari S and Mori M: Roles of CHOP/GADD153 in endoplasmic reticulum stress. Cell Death Differ 11: 381-389, 2004.
11. Nozaki S, Sledge GW Jr and Nakshatri H: Repression of GADD153/CHOP by NF-kappaB: a possible cellular defense against endoplasmic reticulum stress-induced cell death. Oncogene 20: 2178-2185, 2001.
12. McCullough KD, Martindale JL, Klotz LO, Aw TY and Holbrook NJ: Gadd153 sensitizes cells to endoplasmic reticulum stress by down-regulating Bcl2 and perturbing the cellular redox state. Mol Cell Biol 21: 1249-1259, 2001.
13. Hogstrand K, Hejll E, Sander B, Rozell B, Larsson LG and Grandien A: Inhibition of the intrinsic but not the extrinsic apoptosis pathway accelerates and drives MYC-driven tumorigenesis towards acute myeloid leukemia. PLoS One 7: e31366, 2012.
14. Poellinger L and Lendahl U: Modulating Notch signaling by pathway-intrinsic and pathway-extrinsic mechanisms. Curr Opin Genet Dev 18: 449-454, 2008.
15. Harding HP and Ron D: Endoplasmic reticulum stress and the development of diabetes: a review. Diabetes 51 (Suppl 3): S455-S461, 2002.
16. Muhlethaler-Mottet A, Bourloud KB, Auderset K, Joseph JM and Gross N: Drug-mediated sensitization to TRAIL-induced apoptosis in caspase-8-complemented neuroblastoma cells proceeds via activation of intrinsic and extrinsic pathways and caspase-dependent cleavage of XIAP, Bcl-xL and RIP. Oncogene 23: 5415-5425, 2004.
17. Chong ZZ, Kang JQ and Maiese K: Erythropoietin fosters both intrinsic and extrinsic neuronal protection through modulation of microglia, Akt1, Bad, and caspase-mediated pathways. Br J Pharmacol 138: 1107-1118, 2003.
18. Perrin FE, Boisset G, Lathuiliere A and Kato AC: Cell death pathways differ in several mouse models with motoneurone disease: analysis of pure motoneurone populations at a presymptomatic age. J Neurochem 98: 1959-1972, 2006.
19. Kim MK, Kim HS, Lee IK and Park KG: Endoplasmic reticulum stress and insulin biosynthesis: a review. Exp Diabetes Res 2012: 509437, 2012.
20. Gregor MF and Hotamisligil GS: Thematic review series: Adipocyte Biology. Adipocyte stress: the endoplasmic reticulum and metabolic disease. J Lipid Res 48: 1905-1914, 2007.
21. Chakrabarti A, Chen AW and Varner JD: A review of the mammalian unfolded protein response. Biotechnol Bioeng 108: 2777-2793, 2011.
22. Shore GC, Papa FR and Oakes SA: Signaling cell death from the endoplasmic reticulum stress response. Curr Opin Cell Biol 23: 143-149, 2011.
23. Endo H, Murata K, Mukai M, Ishikawa O and Inoue M: Activation of insulin-like growth factor signaling induces apoptotic cell death under prolonged hypoxia by enhancing endoplasmic reticulum stress response. Cancer Res 67: 8095-8103, 2007.
24. Obeng EA and Boise LH: Caspase-12 and caspase-4 are not required for caspase-dependent endoplasmic reticulum stress-induced apoptosis. J Biol Chem 280: 29578-29587, 2005.
25. Wang L, Song R, Shen Y, *et al*: Targeting sarcoplasmic/endoplasmic reticulum Ca^{2+}-ATPase 2 by curcumin induces ER stress-associated apoptosis for treating human liposarcoma. Mol Cancer Ther 10: 461-471, 2011.
26. Wu Z, Liang F, Hong B, *et al*: An endoplasmic reticulum-bound Ca(2+)/Mn(2+) pump, ECA1, supports plant growth and confers tolerance to Mn(2+) stress. Plant Physiol 130: 128-137, 2002.
27. Lai YY, Huang LJ, Lee KH, *et al*: Synthesis and biological relationships of 3',6-substituted 2-phenyl-4-quinolone-3-carboxylic acid derivatives as antimitotic agents. Bioorg Med Chem 13: 265-275, 2005.
28. Lee HZ, Lin WC, Yeh FT and Wu CH: 2-Phenyl-4-quinolone prevents serotonin-induced increases in endothelial permeability to albumin. Eur J Pharmacol 354: 205-213, 1998.
29. Lee HZ: Inhibitory effect of 2-phenyl-4-quinolone on serotonin-mediated changes in the morphology and permeability of endothelial monolayers. Eur J Pharmacol 335: 245-254, 1997.
30. Wang JP, Hsu MF, Raung SL and Kuo SC: Suppressive effect of 2-phenyl-4-quinolone (YT-1) on hind-paw edema and cutaneous vascular plasma extravasation in mice. Naunyn Schmiedebergs Arch Pharmacol 349: 324-330, 1994.
31. Huang SM, Yang JS, Tsai SC, *et al*: The novel synthesized 2-(3-(methylamino)phenyl)-6-(pyrrolidin-1-yl)quinolin-4-one (Smh-3) compound induces G2/M phase arrest and mitochondrial-dependent apoptotic cell death through inhibition of CDK1 and AKT activity in HL-60 human leukemia cells. Int J Oncol 38: 1357-1364, 2011.
32. Ni CH, Chen PY, Lu HF, *et al*: Chrysophanol-induced necrotic-like cell death through an impaired mitochondrial ATP synthesis in Hep3B human liver cancer cells. Arch Pharm Res 35: 887-895, 2012.
33. Tsai SC, Yang JS, Peng SF, *et al*: Bufalin increases sensitivity to AKT/mTOR-induced autophagic cell death in SK-HEP-1 human hepatocellular carcinoma cells. Int J Oncol 41: 1431-1442, 2012.
34. Hour MJ, Tsai SC, Wu HC, *et al*: Antitumor effects of the novel quinazolinone MJ-33: inhibition of metastasis through the MAPK, AKT, NF-kappaB and AP-1 signaling pathways in DU145 human prostate cancer cells. Int J Oncol 41: 1513-1519, 2012.
35. Wu PP, Chung HW, Liu KC, *et al*: Diallyl sulfide induces cell cycle arrest and apoptosis in HeLa human cervical cancer cells through the p53, caspase- and mitochondria-dependent pathways. Int J Oncol 38: 1605-1613, 2011.
36. Huang WW, Ko SW, Tsai HY, *et al*: Cantharidin induces G2/M phase arrest and apoptosis in human colorectal cancer colo 205 cells through inhibition of CDK1 activity and caspase-dependent signaling pathways. Int J Oncol 38: 1067-1073, 2011.
37. Yaguchi T, Saito M, Yasuda Y and Nishizaki T: Caspase-4 activation in association with decreased adenosine deaminase activity may be a factor for gastric ulcer. Digestion 81: 62-67, 2010.

38. Wu SH, Hang LW, Yang JS, *et al*: Curcumin induces apoptosis in human non-small cell lung cancer NCI-H460 cells through ER stress and caspase cascade- and mitochondria-dependent pathways. Anticancer Res 30: 2125-2133, 2010.
39. Huang WW, Chiu YJ, Fan MJ, *et al*: Kaempferol induced apoptosis via endoplasmic reticulum stress and mitochondria-dependent pathway in human osteosarcoma U-2 OS cells. Mol Nutr Food Res 54: 1585-1595, 2010.
40. Huang WW, Yang JS, Lin MW, *et al*: Cucurbitacin E induces G(2)/M phase arrest through STAT3/p53/p21 signaling and provokes apoptosis via Fas/CD95 and mitochondria-dependent pathways in human bladder cancer T24 cells. Evid Based Complement Alternat Med 2012: 952762, 2012.
41. Wu RC, Yu CS, Liu KC, *et al*: Citosol (thiamylal sodium) triggers apoptosis and affects gene expressions of murine leukemia RAW 264.7 cells. Hum Exp Toxicol 31: 771-779, 2012.
42. Lin JP, Yang JS, Chang NW, *et al*: GADD153 mediates berberine-induced apoptosis in human cervical cancer Ca ski cells. Anticancer Res 27: 3379-3386, 2007.
43. Lu HF, Hsueh SC, Ho YT, *et al*: ROS mediates baicalin-induced apoptosis in human promyelocytic leukemia HL-60 cells through the expression of the Gadd153 and mitochondrial-dependent pathway. Anticancer Res 27: 117-125, 2007.
44. Chambers KT, Unverferth JA, Weber SM, Wek RC, Urano F and Corbett JA: The role of nitric oxide and the unfolded protein response in cytokine-induced beta-cell death. Diabetes 57: 124-132, 2008.
45. Kim R, Emi M, Tanabe K and Murakami S: Role of the unfolded protein response in cell death. Apoptosis 11: 5-13, 2006.
46. Lu CC, Yang JS, Chiang JH, *et al*: Novel quinazolinone MJ-29 triggers endoplasmic reticulum stress and intrinsic apoptosis in murine leukemia WEHI-3 cells and inhibits leukemic mice. PLoS One 7: e36831, 2012.
47. Schattenberg JM, Schuchmann M and Galle PR: Cell death and hepatocarcinogenesis: dysregulation of apoptosis signaling pathways. J Gastroenterol Hepatol 26 (Suppl 1): 213-219, 2011.
48. Rosello A, Warnes G and Meier UC: Cell death pathways and autophagy in the central nervous system and its involvement in neurodegeneration, immunity and central nervous system infection: to die or not to die - that is the question. Clin Exp Immunol 168: 52-57, 2012.